Adsorption, 1, 17–27 (1995)

A Simulation Model of a High-Capacity Methane Adsorptive Storage System

J.P. BARBOSA MOTA, E. SAATDJIAN AND D. TONDEUR
Laboratoire des Sciences du Génie Chimique—CNRS, ENSIC, 1 Rue Grandville, B.P. 451, 54001 Nancy Cedex, France

A.E. RODRIGUES*
Lab. of Separation and Reaction Engineering, School of Engineering, University of Porto, 4099 Porto Codex, Portugal

Received March 10, 1994; Revised July 20, 1994; Accepted August 5, 1994

Abstract. A two-dimensional model is developed to describe the hydrodynamics, heat transfer and adsorption phenomena associated with the adsorptive storage of natural gas (NG) in cylindrical reservoirs. Intraparticle and film resistances to both heat and mass transfer are neglected. In the momentum equation, Ergun's law is considered locally valid and is extended to two dimensions. These assumptions are fully justified in the paper. Numerical results are presented concerning the pressurization and blowdown of an ultra-lightweight 50 litre cylinder, commercially available for the storage of compressed NG, if it were filled with an activated carbon having a good adsorptive storage capacity. A simple formula is also proposed to predict the filling times for fast charges. The predicted temperature changes in the packed-bed are in good agreement with those reported in the literature for an experimental charge/discharge.

Introduction

Natural gas has always been considered as an important replacement for petroleum based fuels. It is cheaper than gasoline and diesel fuel, and can be interchanged with gasoline in spark ignition engines without major modifications. NG vehicles are also environmentally safer than gasoline vehicles producing 99% less CO, 30% less NOx, 96% less HCs, and practically no particulates. Because of a high octane number, high compression engines can run on natural gas without the need for a heavy metal additive such as tetraethyl lead. In fact, NG as a transportation fuel outscores gasoline, diesel and other alternative fuels such as methanol in every aspect except onboard fuel storage (Talu, 1992).

Currently, natural gas must be highly compressed (20 MPa) to be stored compactly on a NG vehicle and dispensed quickly. The equipment needed to accomplish this is expensive and heavy, with the multistage compression facility and high-pressure metering equipment comprising as much as 50% of the capital investment required to convert a fleet to NG operation (Remick and Tiller, 1985). A promising new low-pressure system for storing NG is adsorption storage, which at relatively low pressure (3.5 MPa), achievable by single-stage compression, can provide nearly the same capacity of compressed NG (Matranga et al., 1992). This may change the economics leading to a wide acceptance of NG as a transportation fuel (Talu, 1992).

The storage of NG by adsorption presents two major problems not encountered in compression storage systems. The first problem is related to the shape of the adsorption isotherm, which prevents the system from responding linearly to pressure. For compression storage systems, removal of the first 10% of the fuel results in about the same pressure drop as removal of the last 10%. However, this is not the case with the adsorption systems where the greatest pressure drop occurs with the removal of the first 10% of the fuel and as much as 15–18% of the fuel still remains in storage at atmospheric pressure. The second problem is related to both the heat of adsorption which is about 16.7 KJ/mole for methane adsorption on activated carbons, and with the sensitivity of the adsorption isotherm to temperature. During the rapid filling of an adsorption storage system

*Author to whom correspondence should be addressed.

under conditions in which the heat of adsorption is not dissipated, less methane is adsorbed as the substrate heats up. In the discharge process, the temperature drops, thus increasing the residual amount of NG left in the tank at the exhaustion pressure.

Extensive studies indicate that high surface area carbons with high packing density are the best low pressure storage media for NG, proving superior to zeolites (Remick et al., 1984; Talu, 1992). A common performance measure for adsorbed natural gas (ANG) storage is volumes of NG delivered at ambient conditions per storage volume (v/v). Recent Monte Carlo simulations performed by Matranga et al. (1992) for methane adsorption on an idealized carbon during an isothermal filling of the storage tank showed that the maximum theoretical delivered capacity of ANG is 195 v/v for monolithic carbon and 137 v/v for pelletized carbon. The highest experimental values obtained to date are 86 v/v for granular carbon and 125 v/v for monolithic carbon (Quinn, 1990), which have already exceeded the limiting values of 78 v/v for light-duty vehicles and 120 v/v for heavy-duty vehicles, which make ANG more competitive than compressed NG alone (Talu, 1992).

The present work concerns the presentation and study of a two-dimensional model describing the hydrodynamics, heat transfer and adsorption phenomena associated with the adsorptive storage of NG in cylindrical reservoirs filled with high surface area carbons having good storage capacity.

Theoretical Model

Figure 1 illustrates the system under study here. It consists in a cylindrical tank filled with an homogeneous packed-bed of porous adsorbent particles. The gas enters and leaves the tank through the small opening located in the centre of the front face of the cylinder. Due to the tank geometry the problem is clearly two-dimensional and is best described in cylindrical coordinates (z, r). The two-dimensionality of the flow is due mainly to the constriction at the tank entrance. If the process is not adiabatic (e.g. a slow filling) the heat losses through the walls contribute to the 2-D character of the temperature field. NG consists primarily of methane (85–95%), and for vehicular applications one might expect NG to undergo some sort of purification process in order to increase its energy density, so as a first approximation NG is assumed to be pure methane.

The present work concentrates on the dynamics of the packed-bed rather than on the kinetics of the particles, the former being significant only when the particles are sufficiently small. Thus, a simple and reasonable approach to the problem is considering a local equilibrium model, i.e. neglecting all the intraparticle and film resistances to both heat and mass transfer, which also renders the numerical solution more tractable. These are reasonable simplifications at least for the intraparticle resistances. Notice that there is no mass transfer film resistance because we are dealing with a single component.

Based on these assumptions the mass balance (continuity equation) may be written as

$$\frac{\partial}{\partial t}(\epsilon_t c + \rho_b q) + \nabla \cdot \mathbf{G} = 0. \tag{1}$$

For the P–T ranges of study (0–3.5 MPa, 10–90°C) the average value of the methane compressibility factor is 0.97, which allows us to relate the gas concentration c to the pressure and temperature by the ideal gas law:

$$c = P M_g/(R T). \tag{2}$$

The concentration q of the adsorbed phase is determined from the adsorption isotherm:

$$q = f_{\text{eq}}(P, T). \tag{3}$$

In the momentum equation, Ergun's law (Ergun, 1952) is considered locally valid and is extended to two dimensions. Other authors have followed the same approach (e.g. Parsons and Porter, 1992). Recently, Sereno and Rodrigues (1993) studied the influence of several terms of the unsteady-state momentum equation and concluded that the simpler steady-state form can be safely used in modelling the pressurization of adsorbers. Since these authors used a 1-D model for the comparisons, they were unable to test the additional viscous term ($\mu \nabla^2 \mathbf{v}$) introduced by Brinkman (1947; also Vafai and Tien, 1981), which accounts for the presence of a solid boundary. However, this term is only significant when the bed-particle diameter ratio is small (<10) or when detailed boundary layer studies are needed.

The vectorial form of Ergun's equation, when solved for the superficial mass velocity vector, can be expressed as follows:

$$\mathbf{G} = -\frac{2c\nabla P}{\alpha + \sqrt{\alpha^2 + 4\beta c \|\nabla P\|}}, \tag{4}$$

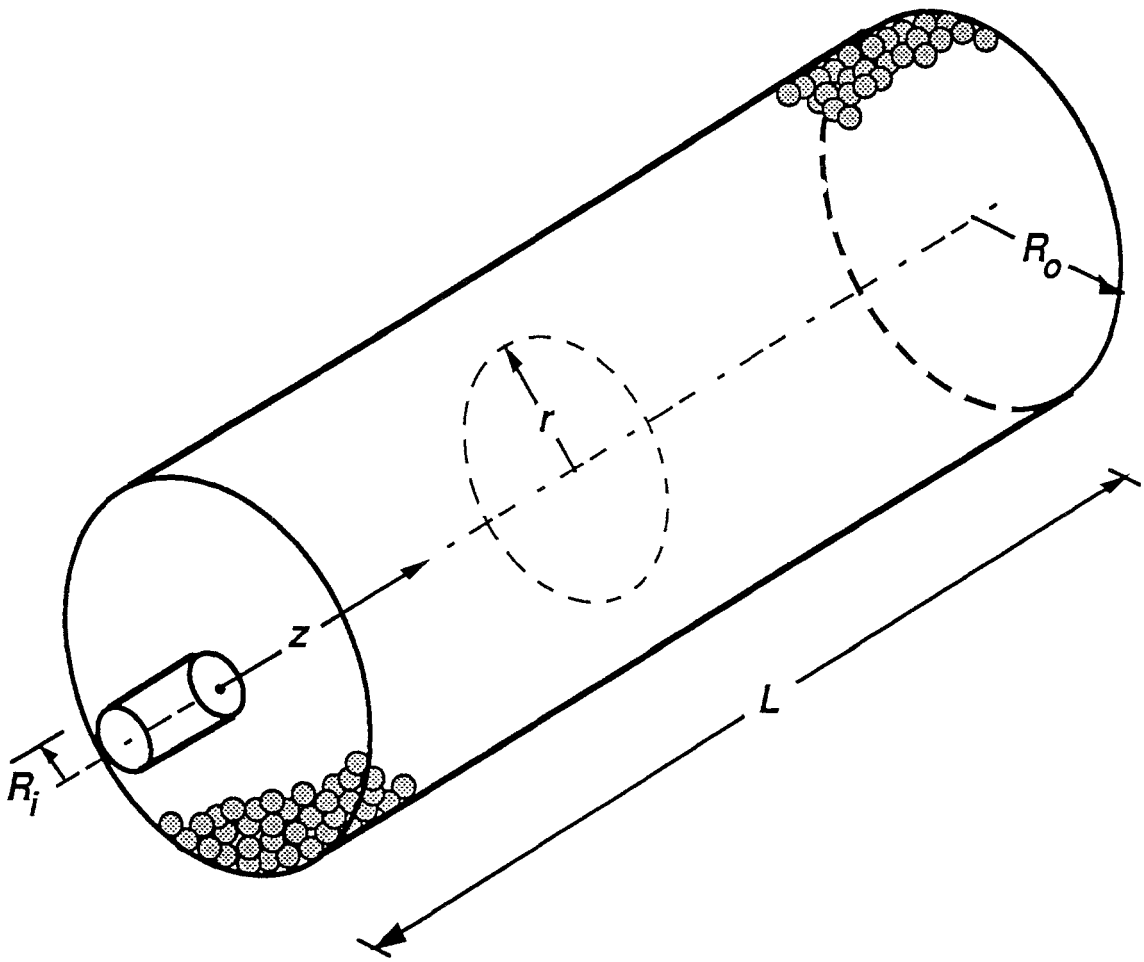

Fig. 1. Schematic diagram of the reservoir and coordinate system.

where

$$\alpha = 150(1-\epsilon)^2\mu/(\epsilon^3 d_p^2),$$
$$\beta = 1.75(1-\epsilon)/(\epsilon^3 d_p), \tag{5}$$

and $\|\nabla P\| = \sqrt{(\partial P/\partial z)^2 + (\partial P/\partial r)^2}$ is the pressure gradient modulus. The energy equation considered here is

$$\frac{\partial}{\partial t}((\epsilon_t c + \rho_b q)C_{pg}T) + \rho_b \Delta H \frac{\partial q}{\partial t} - \frac{\partial P}{\partial t} + \rho_b C_{ps}\frac{\partial T}{\partial t} + \nabla \cdot (\mathbf{G}C_{pg}T - \lambda_e \nabla T) = 0, \tag{6}$$

and is based on the assumption of negligible rates of change of kinetic and potential energy of the gas when compared with the rate of change of the system's internal energy. Also, mean values were considered for the isosteric heat of adsorption (ΔH) and for the thermodynamic properties of the gas and solid. While this assumption may be a gross approximation for the heat of adsorption it is a reasonable one for the other thermodynamic properties, e.g. the maximum difference between the average value considered and the true value is 10% for the viscosity and 8% for the heat capacity of the gas. The compression work, which has rarely been considered in PSA models, has been taken into account in the energy equation since it is not negligible when the pressure ratio is high (Lu et al., 1992). Notice that Eq. (6) is written in conservative form since it is a requirement of the numerical method used to solve the problem.

The initial conditions are

$$P = P_i, \quad T = T_i \quad \text{for } 0 \le z \le L,\ 0 \le r \le R_0,\ t = 0. \tag{7}$$

The pressure boundary condition at the walls states that the normal component of velocity vector is null at those points:

$$G_z = 0 \text{ for } \begin{cases} z = 0,\ R_i \le r \le R_0 \\ z = L,\ 0 \le r \le R_0,\ t > 0. \end{cases} \quad (8)$$
$$G_r = 0 \text{ for } \quad r = R_0,\ 0 \le z \le L$$

The temperature boundary condition states that all the heat flux through the walls occurs by conduction:

$$\begin{aligned} &\lambda_e(\partial T/\partial z) = h_w(T - T_w) \\ &\quad \text{for} \quad z = 0,\ R_i \le r \le R_0 \\ &\lambda_e(\partial T/\partial z) = h_w(T_w - T) \\ &\quad \text{for} \quad z = L,\ 0 \le r \le R_0,\ t > 0. \\ &\lambda_e(\partial T/\partial r) = h_w(T_w - T) \\ &\quad \text{for} \quad r = R_0,\ 0 \le z \le L \end{aligned} \quad (9)$$

On the longitudinal axis there is the symmetry condition:

$$\frac{\partial P}{\partial r} = 0, \quad \frac{\partial T}{\partial r} = 0 \quad \text{for} \quad 0 \le z \le L,\ r = 0,\ t > 0. \quad (10)$$

In the opening the following boundary conditions are used:

$$P = P_{\text{ext}}, \quad \begin{matrix} -(L/Pe_z)\partial T/\partial z + T = T_{\text{ext}} \\ \text{(during charge)} \\ \partial T/\partial z = 0 \\ \text{(during discharge)} \end{matrix}$$
$$z = 0,\ 0 \le r \le R_i,\ t > 0, \quad (11)$$

where Pe_z is the axial Peclet number. In (11) we are specifying the pressure at the entrance and neglecting the conductive heat flux. The temperature boundary condition is perhaps best understood by rewriting it in the more concise form:

$$\begin{aligned} Q &= G_z C_{pg} T^*, \\ T^* &= \begin{cases} T_{\text{ext}} & \text{for} \quad G_z > 0 \\ T & \text{for} \quad G_z < 0 \end{cases}, \\ z &= 0,\ 0 \le r \le R_i,\ t > 0, \end{aligned} \quad (12)$$

where Q represents the energy flux through the opening. For pressurizations (12) quickly becomes $T = T_{\text{ext}}$, whereas for blowdowns it behaves like an open boundary condition.

Solution Method

Equations (1–6) together with the initial and boundary conditions (7–12) were solved numerically using a package developed by the authors for the solution of systems of partial differential equations (PDEs), which in vector form may be written as

$$\mathbf{f}(t, x, y, \phi, \phi', \mathbf{u}) + \nabla \cdot \mathbf{u}(t, x, y, \phi, \nabla\phi) = 0 \quad \text{in} \quad \Omega \quad \text{for} \quad t \ge 0, \quad (13)$$

where x and y represent general spatial coordinates, $\mathbf{u} = \mathbf{u}_x\mathbf{e}_x + \mathbf{u}_y\mathbf{e}_y$ denotes the flux vectors and ϕ is the n vector holding the dependent variables, n being the number of PDEs. The boundary of the domain Ω is divided into arbitrary nonoverlapping zones (say $\partial\Omega_k, k = 1, \ldots, m$), each having mixed boundary conditions of the type

$$w_i^k(t, x, y, \phi, \phi') = 0 \quad \text{or} \quad u_i = w_i^k(t, x, y, \phi, \phi') \quad \text{in} \quad \partial\Omega_k, \quad i = 1, \ldots, n. \quad (14)$$

In the present case the PDE system is given by Eqs. (1) and (6) and $\phi = (P,\ T)$. The boundaries of the tank were divided into 4 zones according to the different boundary conditions: opening, front face excluding the opening, lateral wall, and rear face.

The methodology adopted in the package follows the *Numerical Method of Lines* (NUMOL) approach (Schiesser, 1991), but was inspired to a great extent by the classical control-volume formulation proposed by Patankar (1980). A portion of the two-dimensional grid is shown in Fig. 2, where the control-volume associated with point (i, j) is represented by dashed lines. The control-volume faces are located midway between the neighboring grid points, this leads to half control-volumes near the boundaries and quarter control-volumes at the corners. Due to the conservative form of Eq. (12), its integration over the control-volume results in a relation between the fluxes normal to the faces, which we approximate by

$$\begin{aligned} &(V\mathbf{f})_{i,j} + (A^x\mathbf{u}_x)_{i+1/2,j} + (A^y\mathbf{u}_y)_{i,j+1/2} \\ &\quad - (A^x\mathbf{u}_x)_{i-1/2,j} - (A^y\mathbf{u}_y)_{i,j-1/2} = 0, \end{aligned} \quad (15)$$

where $V_{i,j}$ is the volume of the control-volume and the As are the areas of the control-volume faces (see Fig. 2). The subscripts indicate where the quantities are evaluated. The fluxes are discretized using second order centered finite differences, with the exception of the convective term in the energy equation ($\mathbf{G}C_{pg}T$),

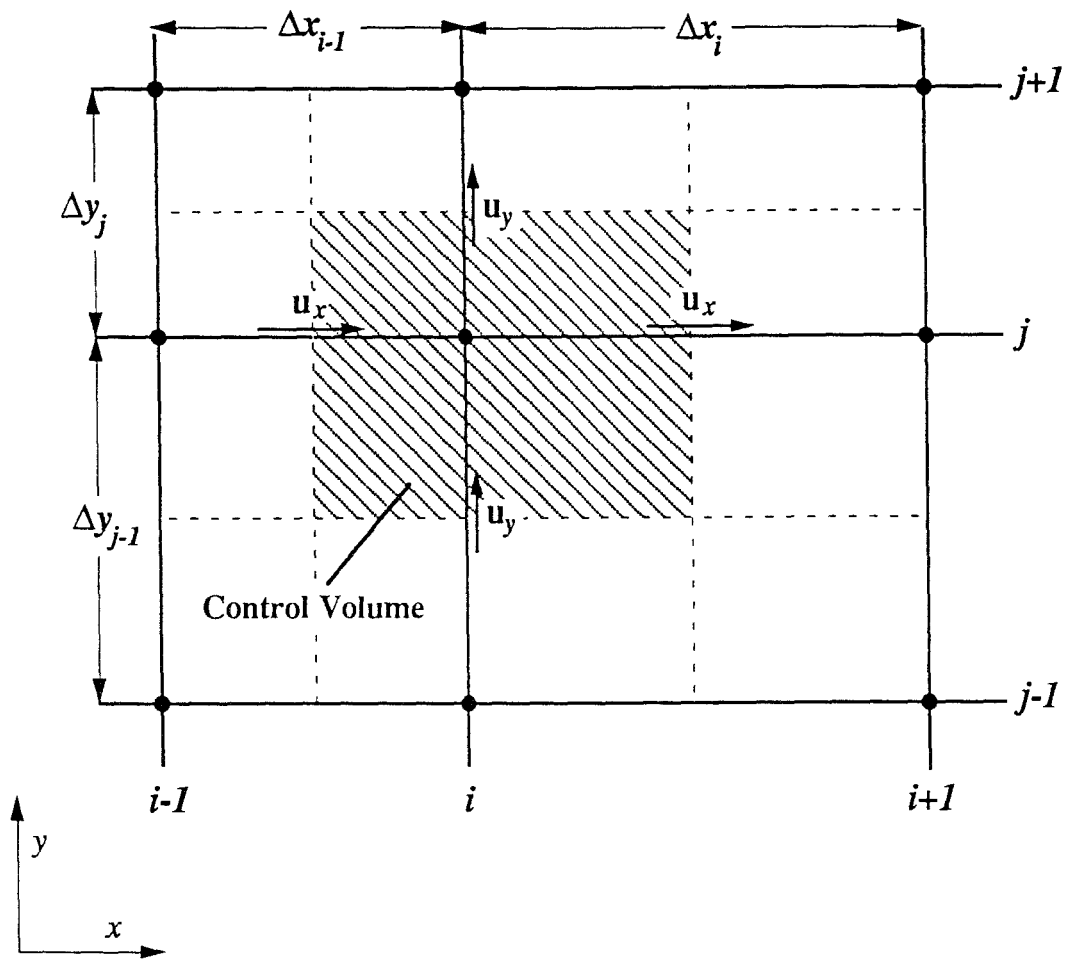

Fig. 2. Portion of the two-dimensional grid showing the control-volume around point (i, j).

which is discretized using the skew upstream differencing scheme proposed by Raithby (1976) in order to avoid a possible unphysical oscillatory behaviour of the thermal field in the regions where convection strongly dominates diffusion.

The resulting system of ordinary differential equations is solved using the stiff code DASSL of Petzold (1983) which uses a variable stepsize variable order implementation of the *backward differentiation formulas* (Gear, 1971; Brenan et al., 1989). However, DASSL has to be modified in several ways in order to be used efficiently in the NUMOL context. A critical point is the method employed in the solution of the linear systems of algebraic equations generated by the integrator at each time step. Since the finite-volume method relates each grid point with the 8 neighboring points surrounding it, the linear systems have a nine-diagonal block structure. We have replaced the LINPACK band matrix solver included in DASSL by an extension of the iterative *Modified Strongly Implicit Procedure* by Schneider and Zedan (1981). This method was originally proposed for the solution of the linear systems resulting from the discretization of a single equation. To our knowledge we are the first ones to extended the method to the linear systems resulting from the discretization of several equations. The method has a high convergence rate and modest storage requirements.

Results and Discussion

The reservoir considered in the simulations is an ultra-lightweight NGV 50 litre cylinder (87 cm × 30 cm, 13 Kg), manufactured by EDO Canada Ltd. and designed to store compressed NG at a maximum operating pressure of 20.7 MPa. Figure 3 shows the

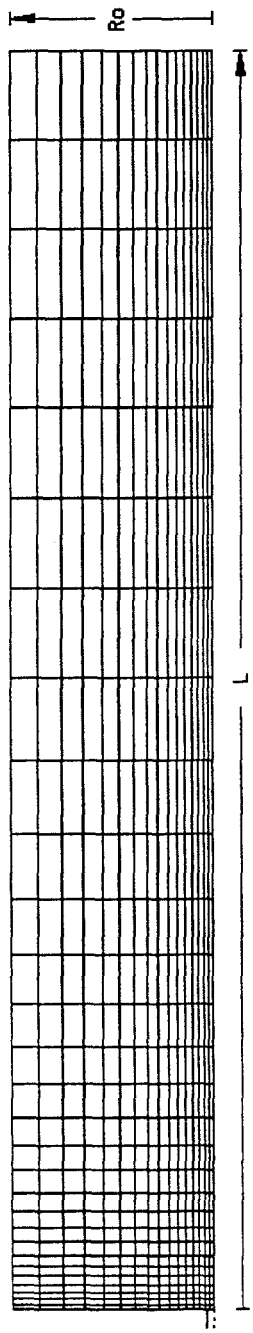

Fig. 3. Computational grid (30 × 17 points).

nonuniform mesh used in the simulations, consisting in 30 × 17 ($z \times r$) grid points which were more concentrated near the opening where the steepest gradients occur.

The axial and radial components of the effective thermal conductivity tensor were considered equal

Table 1. Data used in the numerical simulations.

$C_{pg} = 2450$ J kg^{-1} K^{-1}	$R_0 = 0.14$ m
$C_{ps} = 648$ J kg^{-1} K^{-1}	$T_{\text{ext}} = 283$ K
$\Delta H = -1.1 \times 10^{-6}$ J kg^{-1}	$T_i = 283$ K
$h_w = 0.0$ J m^{-1} s^{-1}	$T_w = 283$ K
$L = 0.85$ m	$\lambda_g = 4.24 \times 10^{-2}$ J m^{-1} s^{-1}
$M_g = 16.04 \times 10^{-3}$ kg mol^{-1}	$\lambda_s = 164.4$ J m^{-1} s^{-1}
$P_{\text{ext}} = 3.45/0.101$ MPa	$\mu = 1.26 \times 10^{-5}$ kg m^{-1} s^{-1}
$P_i = 0.0/3.45$ MPa	$\rho_s = 2150$ kg m^{-3}
$R_i = 0.005$ m	

and given by

$$\lambda_{ez} = \lambda_{er} = \lambda_e^0 + \gamma C_{pg} d_p \|\mathbf{G}\|, \quad \gamma = 0.3, \tag{16}$$

with the static contribution λ_e^0 taken from the correlation given by Zehner and Schlunder (1970, 1972). The equilibrium relation used in this work is of Langmuir type, and is based on the experimental data published by Remick and Tiller (1986) for an activated carbon having a good NG storage capacity:

$$q = \frac{q_m b P}{1 + bP}, \quad q_m = 55920\, T^{-2.3},$$
$$b = 1.0863 \times 10^{-7} e^{806/T}. \tag{17}$$

There was a need to set the saturation limit q_m dependent on temperature in order to obtain a good adjustment to the 2 experimental isotherms (25°C and 90°C). The values of the fluid, particle and system properties used in the numerical simulations are listed in Table 1. For simplicity the tank was assumed adiabatic (i.e. $h_w = 0$), which is a good approximation for the case of fast fillings. Both cases of porous ($\epsilon_p = 0.6$) and nonporous particles were studied, and in the former case with and without adsorption. The bed porosities considered were $\epsilon = \{0.2, 0.3, 0.4, 0.5\}$; the particle diameters were 0.2, 1 and 5 mm. The loading pressure was 3.45 MPa, with the system being charged from vacuum in the pressurizations and the exhaustion pressure being 0.101 MPa for the discharges.

Figure 4 shows the pressure field at two different times for one of the runs, and illustrates the transient behaviour of the pressure field for all the pressurizations simulated. The main pressure drop is located in a small region surrounding the opening, here the gas velocity decreases rapidly due to the sudden expansion and the frictional drag. The decrease in velocity reduces the pressure drop allowing the rest of the cylinder to fill uniformly.

As the gas expands near the opening its temperature decreases. However, the rest of the gas heats up

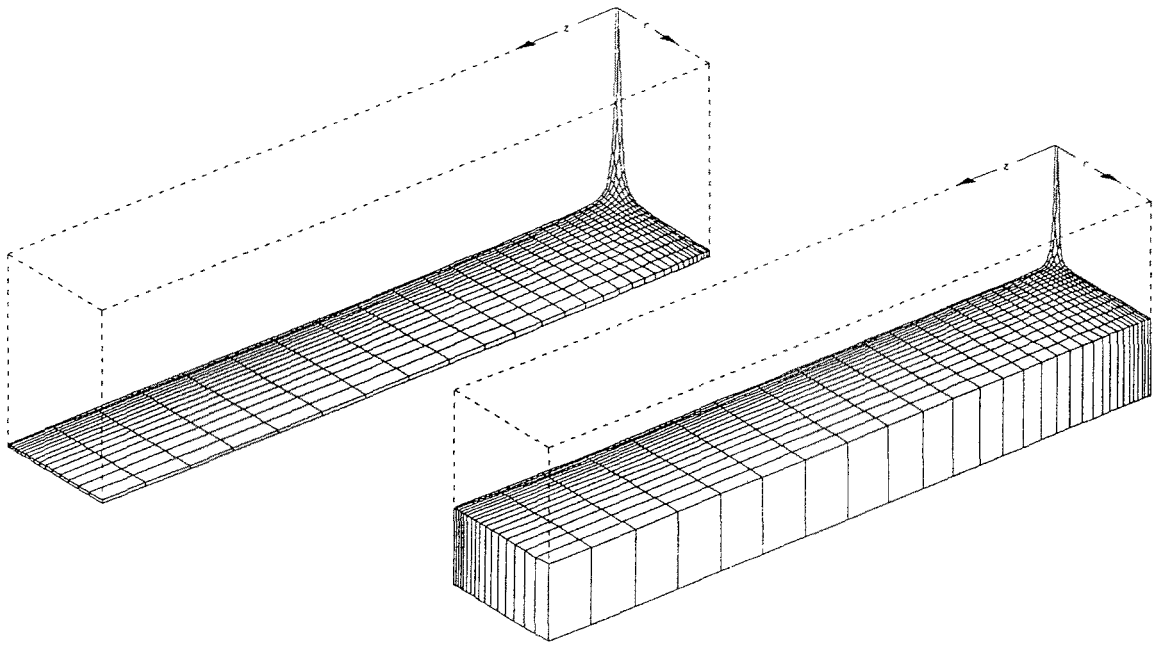

Fig. 4. Pressure field during pressurization with adsorbing particles ($\epsilon = 0.3$, $\epsilon_p = 0.6$, $d_p = 1$ mm) left: $t = 6.9$ s, right: $t = 29.7$ s. In each picture: bottom plane = 0.0 MPa, top plane = 3.45 MPa.

since we are dealing with a pressurization, and the overall effect will be an increase in the temperature of the system. This situation is best depicted in Fig. 5 corresponding to a run without adsorption.

If the gas adsorbs in the particles the undissipated heat of adsorption does not increase the bed temperature near the opening, this is due to the higher expansion ratio. The gas that is not adsorbed acts as if it had a higher free volume to expand than the true bed void volume, the excess being the volume occupied by the adsorbed phase if it were in the gaseous state. In the rest of the bed the temperature raises significantly (Fig. 6).

A good estimate of the adiabatic rise in temperature can be obtained without the need to solve the PDE system in detail. Integrating the continuity and energy equations over the tank volume and from the initial time $t_i = 0$ up to the end of the pressurization t_{end}, yields:

$$\begin{aligned}\Delta_V \; & ((\epsilon_t c + \rho_b q) C_{pg} T + \rho_b \Delta H q \\ & - P + \rho_b C_{ps} T)) \\ & = C_{pg} T_{\text{ext}} \Delta_V (\epsilon_t c + \rho_b q). \end{aligned} \tag{18}$$

The operator $\Delta_V(\cdot)$ is defined as

$$\Delta_V(\phi) = \int\int\int_V \phi_{\text{end}} dV - V\phi_i$$

$$= V(\overline{\phi}_{\text{end}} - \phi_i), \tag{19}$$

where the bar represents the average over the tank volume V. If one makes the approximation: $\overline{\phi}_{\text{end}} = \phi(P_{\text{ext}}, \overline{T}_{\text{end}})$, then the nonlinear Eq. (18) can be solved by any standard iterative method for $\overline{T}_{\text{end}}$. This gives temperature rises of 1.6°C, 7.7°C and 78.8°C for the three cases considered: both porous and nonporous particles without adsorption, and the porous adsorbing particles. The last result is in agreement with the experimental temperature rise of 82°C, reported by Remick and Tiller (1986), for the fast filling of a one litre cylinder filled with the same carbon.

The results suggest that the filling time for fast charges depends on the diameter of the opening and on the volume of the tank, but not on the tank geometry. This is due to most of the pressure drop being concentrated around the opening and not being directly influenced by the walls of the cylinder. An analysis of the velocity field showed that during the pressurizations the gas velocity was sufficiently high to make the inertial forces dominate over the viscous effects. This leads us to consider a reference mass flow defined by

$$\widetilde{G}_m = (\pi R_i^2)\sqrt{c_{\text{ext}}(P_{\text{ext}} - P_i)/(\beta\zeta)}, \tag{20}$$

where ζ is a length yet to be determined. The total mass of methane (i.e. gas + adsorbed phase) stored at

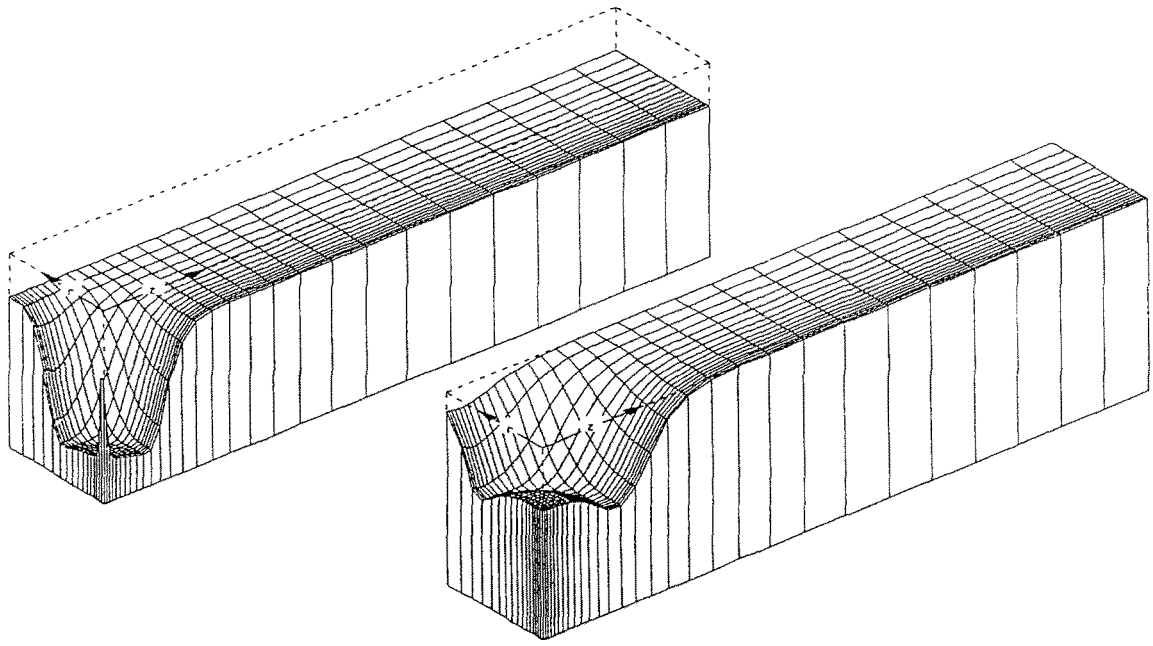

Fig. 5. Temperature field during pressurization with nonadsorbing particles ($\epsilon = 0.3$, $\epsilon_p = 0.6$, $d_p = 1$ mm) left: $t = 5.0$ s, right: $t = 22.4$ s. In each picture: bottom plane $= -3.2°C$, top plane $= 16.7°C$.

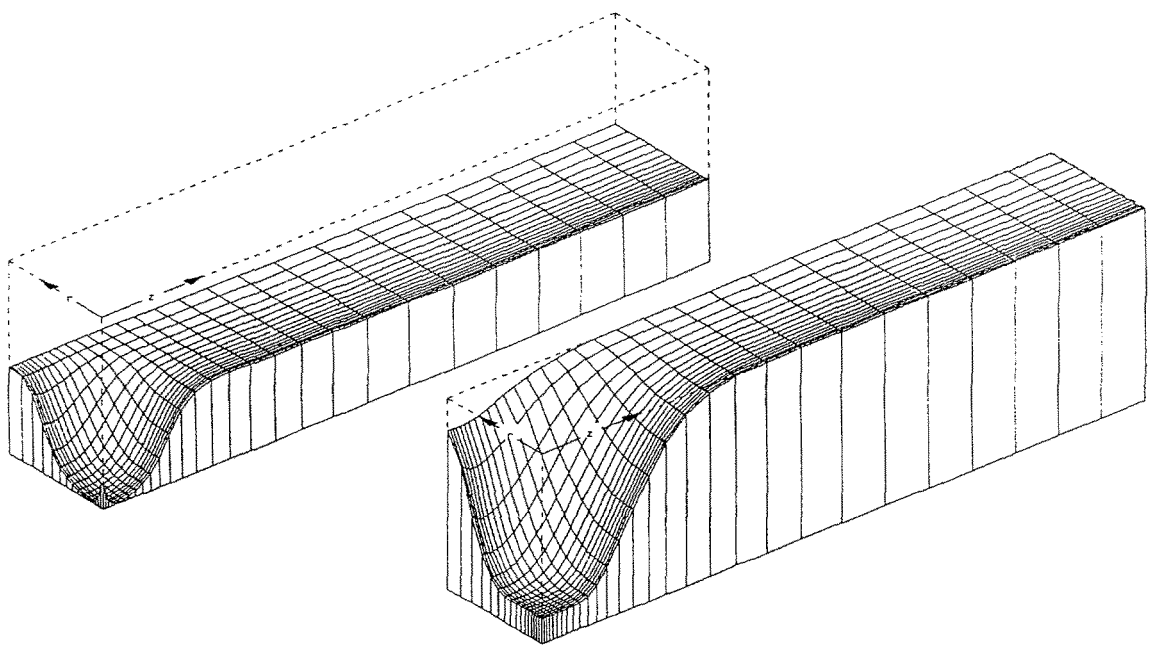

Fig. 6. Temperature field during pressurization with adsorbing particles ($\epsilon = 0.3$, $\epsilon_p = 0.6$, $d_p = 1$ mm) left: $t = 10.4$ s, right: $t = 49.3$ s. In each picture: bottom plane $= -4.0°C$, top plane $= 98.0°C$.

Table 2. Values of ζ (mm).

d_p (mm) \ ϵ	0.2	0.3	0.4	0.5	ϵ_p
	8.17	7.55	7.32	7.21	0.0
0.2	8.13	7.50	7.27	7.18	0.6
	4.98	4.82	4.85	4.97	0.6*
	7.17	7.11	7.14	7.11	0.0
1	7.13	7.08	7.09	7.08	0.6
	4.53	4.62	4.75	4.92	0.6*
	7.12	7.09	7.06	7.05	0.0
5	7.05	7.04	7.09	7.11	0.6
	4.48	4.59	4.74	4.90	0.6*

*Identifies runs considering adsorption.

the end of each pressurization can be estimated as

$$\begin{aligned} W_{\text{end}} &= \pi R_0^2 L(\epsilon_t \bar{c}_{\text{end}} + \rho_b \bar{q}_{\text{end}}), \\ \bar{c}_{\text{end}} &= c(P_{\text{ext}}, \overline{T}_{\text{end}}), \\ \bar{q}_{\text{end}} &= q(P_{\text{ext}}, \overline{T}_{\text{end}}), \end{aligned} \tag{21}$$

with $\overline{T}_{\text{end}}$ determined by the method described earlier. Thus, a suitable reference time is

$$\begin{aligned} \tilde{t}_{\text{end}} &= W_{\text{end}}/\tilde{G}_m \\ &= (R_0/R_i)^2 L(\epsilon_t \bar{c}_{\text{end}} \\ &\quad + \rho_b \bar{q}_{\text{end}})/\sqrt{c_{\text{ext}}(P_{\text{ext}} - P_i)/(\beta\zeta)}. \end{aligned} \tag{22}$$

Table 2 lists the ζ values that match each reference time with the corresponding pressurization time given by the simulations. An average ζ value of 7.24 mm is obtained for the runs without adsorption with a mean relative deviation of 2.8%. For the runs including adsorption the average ζ value is 4.8 mm with mean relative deviation of 3.0%. Given that in Eq. (20) the pressure gradient ∇P is approximated by $(P_{\text{ext}} - P_i)/\zeta$ and according to Fig. 4, ζ can be viewed as an estimate of the mean penetration distance from the opening of the cylinder where the steepest gradients occur.

The discharges were found to be 2.5 to 4.5 times longer than the corresponding filling times for the case of nonadsorbing particles, and from 8 to 20 times longer for the runs with adsorption. Both pressure and temperature gradients inside the tank were negligible. The uniform temperature field is a consequence of the thermicity of the system being much less dependent on the exterior for the discharges than for the pressurizations, in the latter case the temperature of gas entering the cylinder is solely controlled by the exterior. The heat of adsorption released during the pressurization must be resupplied during discharge, otherwise the simulations predict a temperature drop in the bed of 64°C. This is in agreement with the experimental value of 62°C reported by Remick and Tiller (1986).

Conclusions

The charge/discharge characteristics of NG adsorptive storage systems were studied numerically. The results show that the heat of adsorption released during a fast charge increases the bed temperature by 78°C, and if not ressuplied during the discharges lowers the temperature by 64°C. These results are in agreement with the temperature measurements reported by Remick and Tiller (1986).

For vehicular applications, taking the vacuum as the initial condition for the charge cycles is unrealistic (except for the first filling of the reservoir) and a more realistic condition would certainly be the exhaustion pressure used in the discharge cycles. The zero pressure initial condition was used in order to match the experimental conditions employed by Remick and Tiller (1986), since charging from atmospheric pressure would neglect the thermicity effects associated with about 16% of the total methane stored at 3.5 MPa. Qualitatively our simulation results are still valid and the formula proposed for the filling time can be used provided that P_i is changed and $\overline{T}_{\text{end}}$ recalculated from Eq. (18).

ANG vehicles will have controlled discharge rates which are sufficiently low so that the pressure gradients in the tank can be completely neglected. In this case an approach similar to that employed to predict the filling time, coupled with an overall heat transfer coefficient to account for the heat exchange to the surroundings, might be sufficient to reasonably describe the response of the storage system to the energy demand of the vehicle.

Currently the model is being extended by including intraparticle and film resistances to heat and mass transfer, so that one can assess their importance in the dynamics of the process.

Nomenclature

b Parameter of the Langmuir equilibrium relation (Pa^{-1})

C_{pg} Heat capacity of gas at constant pressure ($\text{J kg}^{-1}\ \text{K}^{-1}$)

C_{ps} Heat capacity of the adsorbent ($\text{J kg}^{-1}\ \text{K}^{-1}$)

c Gas concentration (kg m^{-3})
d_p Particle diameter (m)
$\mathbf{G}$ [$= G_z\mathbf{e}_z + G_r\mathbf{e}_r = c\mathbf{v}$] Mass superficial velocity vector (kg m^{-2} s^{-1})
G_m mass flow (kg m^{-2} s^{-1})
H Enthalpy of the gas (J kg^{-1})
ΔH Isosteric heat of adsorption (J kg^{-1})
h_w Effective heat transfer coefficient at the wall (J m^{-1} s^{-1})
L Length of the cylinder (m)
M_g Molecular mass of the gas (kg mol^{-1})
P Pressure (Pa)
Pe_z [$= G_z C_{pg} L/\lambda_e$] Axial Peclet number
Q Energy flux (J m^{-2} s^{-1})
q Concentration of the adsorbed phase (kg kg^{-1})
q_m Saturation limit of the Langmuir equilibrium relation (kg kg^{-1})
R Ideal gas constant (= 8.31441 J mol^{-1} K^{-1})
R_i Radius of the tank opening (m)
R_0 Cylinder radius (m)
r Radial coordinate (m)
T Temperature (K)
T_w Wall temperature (K)
t Time (s)
$\mathbf{v}$ [$= v_z\mathbf{e}_z + v_r\mathbf{e}_r$] Superficial velocity vector (m s^{-1})
z Axial coordinate (m)

Greek Letters

γ Constant
ϵ Bed (interparticle) porosity
ϵ_p Adsorbent (intraparticle) porosity
ϵ_t [$= \epsilon + (1-\epsilon)\epsilon_p$] Total porosity
λ_e Effective thermal conductivity tensor (J K^{-1} m^{-1} s^{-1})
λ_e^0 Static contribution of the effective thermal conductivity tensor (J K^{-1} m^{-1} s^{-1})
λ_{er} radial component of the effective thermal conductivity tensor (J K^{-1} m^{-1} s^{-1})
λ_{ez} axial component of the effective thermal conductivity tensor (J K^{-1} m^{-1} s^{-1})
λ_g Thermal conductivity of the gas (J K^{-1} m^{-1} s^{-1})
λ_s Thermal conductivity of the solid (J K^{-1} m^{-1} s^{-1})
μ Viscosity of the gas (kg m^{-1} s^{-1})
ρ_b [$= (1-\epsilon)(1-\epsilon_p)\rho_s$] Packing (bed) density (kg m^{-3})
ρ_s Density of the solid (kg m^{-3})

Superscripts

$-$ Average value
$\sim$ Reference conditions
$'$ Partial derivative with respect to time

Subscripts

end Conditions at the end of the charge /discharge
ext External gas
i Initial conditions

Acknowledgments

One of the authors (J.P.B.M.) benefits from the financial support of JNICT (Portugal) through grant BD/1607/91-RM.

References

Brenan, K.E., S.L. Campbell, and L.R. Petzold, *Numerical Solution of Initial-Value Problems in Differential-Algebraic Equations*, Elsevier Science Publishing Co., Inc., New York, 1989.

Brinkman, H.C., "A calculation of the viscous force extended by a flowing fluid on a dense swarm of particles," *Appl. Scient. Res.*, **A1**, 27–34 (1947).

Ergun, S., "Fluid flow through packed columns," *Chem. Eng. Prog.*, **42**, 89 (1952).

Gear, C.W., "The simultaneous numerical solution of differential-algebraic equations," *IEEE Trans. Circuit Theory*, **CT-18**, 89–95 (1971).

Lu, Z.P., J.M. Loureiro, M.D. LeVan, and A.E. Rodrigues, "Dynamics of pressurization and blowdown of an adiabatic bed: III," *Gas Sep. & Purif.*, **6**, 15–23 (1992).

Matranga, K.R., A.L. Myers, and E.D. Glandt, "Storage of natural gas by adsorption on activated carbon," *Chem. Eng. Sci.*, **47**, 1569–1579 (1992).

Parsons, I.M. and K.E. Porter, "Gas flow patterns in packed beds: A computational fluid dynamics model for wholly packed domains," *Gas Sep. & Purif.*, **6**, 221–227 (1992).

Patankar, S.V., *Numerical Heat Transfer and Fluid Flow*, Hemisphere Publishing Corp., New York, 1980.

Petzold, L.R., "A Description of DASSL: A differential/algebraic system solver," *Scientific Computing*, R.S. Stepleman et al. (Eds.), North-Holland, Amsterdam, 65–68, 1983.

Quinn, D., *Carbon adsorbents for natural gas*, Presentation to GURF meeting, London, 1990.

Raithby, G.D., "Skew upstream differencing schemes for problems involving fluid flow," *Comput. Methods Appl. Mech. Eng.*, **9**, 153–164 (1976).

Remick, R.J. and A.J. Tiller, "Advanced methods for low-pressure storage of CNG," *The Proceedings of Nonpetroleum Vehicular Fuels Symposium*, pp. 105–119, Chicago, IL, 1985.

Remick, R.J. and A.J. Tiller, "Heat generation in natural gas adsorption systems," in *The Proceedings of the Gaseous Fuels for Transportation International Conference*, Vancouver, Canada, 1986.

Schneider, G.E. and M. Zedan, "A Modified strongly implicit procedure for the numerical solution of field problems," *Numer. Heat Transfer*, **4**, 1–19 (1981).

Sereno, C. and A.E. Rodrigues, "Can steady-state momentum equations be used in modelling pressurization of adsorption beds?" *Gas Sep. & Purif.*, **7**, 167–174 (1993).

Schiesser, W.E., *The numerical method of lines: integration of partial differential equations*, Academic Press Inc., San Diego, CA, 1991.

Talu, O., "An overview of adsorptive storage of natural gas," in *The Proceedings of the 4th International Conference on Fundamentals of Adsorption*, Kyoto, Japan, 1992.

Zehner, P. and E.U. Schlunder, *Chem. Eng. Techn.*, **44**, 1303 (1970); *Chem. Eng. Techn.*, **42**, 333 (1972).